A CALIBRATION PROCEDURE FOR CCD ARRAY CAMERAS

Kerry McIntosh
Department of Civil Engineering and Surveying
University of Newcastle
Australia

Commission I, Working Group 3

KEY WORDS: CCD Cameras, Calibration Method, Close Range

ABSTRACT

The purpose of the research discussed in this paper is to use the knowledge gained from reviewing existing calibration techniques to develop a versatile calibration procedure to be used for several different types of CCD array cameras. The procedure developed was required to be flexible in order to handle different types of digital cameras, and thorough to provide complete calibration information so the cameras could be used as precise measurement tools. A major component in the calibration procedure was the use of a bundle adjustment to process the observations produced from the measurements of a target plate. The procedure was applied to calibrate four cameras to be used in close-range photogrammetric applications.

1. INTRODUCTION

There are many calibration techniques and methods which have been developed for use in close-range photogrammetric applications (*for example:* Beyer, 1992, Burner *et al.*, 1990; Curry *et al.*, 1986; Fryer & Fraser, 1986; Lenz, 1987; Michael, 1992; Shortis *et al.*, 1995b; Wong & Obaidat, 1994). All have varying degrees of complexity and suitability to different applications and cameras. This paper describes a camera calibration procedure, including hardware and software, which has been developed specifically to handle a variety of cameras.

Several CCD cameras had been acquired by the University of Newcastle's photogrammetric laboratory by 1995, but none of the cameras had been thoroughly calibrated. A procedure was required to allow all the cameras to be thoroughly and easily calibrated, accommodating different image acquisition methods, varying focal lengths and object distances.

The camera calibration procedure which was developed was based on a rigorous bundle adjustment incorporating a comprehensive set of calibration parameters appropriate to CCD cameras. The calibration parameters which were determined included lens distortions (radial and decentering), the offsets of the principal point and coefficients which represent any shear effects in the CCD array and the tilt of the CCD array around its X and Y axes. The radiometric characteristics of the cameras were also investigated and were corrected where necessary.

A target plate was manufactured and coordinated so each target had accurately known coordinates. The targets were made from retro-reflective material to provide the best contrast to the black background of the target plate. Images of the target plates were acquired with each camera and observations to the targets were made using a PC-based program. The image coordinates of the centre of each target were determined in the program by centroiding.

The observations were processed using a least-squares bundle adjustment. The parameters for decentering distortion were determined prior to the bundle adjustment by the plumbline method of lens calibration (See Fryer & Brown, 1986, and Shortis, 1995a). The decentering distortion parameters are highly correlated to the offsets of the principal point and were constrained accordingly in the bundle adjustment to allow the offsets of the principal point to be determined.

2. CAMERAS

The cameras included two digital still cameras and two analog video cameras. The digital still cameras were from different companies (Logitech & Apple) although Table 1 below indicates their characteristics were almost identical. It has been noted that the Kodak DC-40 is also very similar to these cameras. However, they have different image storage capacities and techniques. The two video cameras (both Philips) are used in conjunction with a PC-Vision*Plus* frame grabber and are usually used as a stereo pair, but for this research, they were calibrated individually.

Camera	Type	Pixel Size (μm)	Array Size (pixels)	Array Size (mm)
Apple Quicktake	Digital still	9 x 9	768 x 512	6.9 x 4.6
Logitech Fotoman	Digital still	9 x 9	768 x 512	6.9 x 4.6
Left Philips **	Analog video	9.9 x 7.6	604 x 588	6.0 x 4.5
Right Philips **	Analog video	9.9 x 7.6	604 x 588	6.0 x 4.5
**Frame Grabber	Used with both Philips	11.6 x 7.6	512 x 512	

Table 1. Camera Specifications.

3. CORRECTIONS

3.1 Geometric Corrections

The geometric characteristics investigated in this calibration procedure include lens distortions (radial and decentering), offsets of the principal point and additional parameters which represented the effects of shear and tilt of the CCD sensor array. Mathematical models for these geometric characteristics are given below.

3.1.1 Radial Lens Distortion: Radial lens distortion ,δr, is mathematically represented by a polynomial function of the radial distance r (Fryer & Brown, 1986 and Karara, 1989) where

$$\delta r = K_1\ r^3 + K_2\ r^5 + K_3\ r^7 + \ldots \quad (1)$$

where K_1 and K_2 were the terms determined during the bundle adjustment. K_3 was considered to be insignificant for the simple lenses used on inexpensive video cameras and assumed to be zero. Also

$$r^2 = (x - x_p)^2 + (y - y_p)^2 \quad (2)$$

where x and y are image coordinates and x_p and y_p are offsets of the principal point. Figures 2 and 4 in Section 5 graph the results of Equation 1 produced from the bundle adjustments.

3.1.2 Decentering Lens Distortion: The decentering distortion equations follow the derivation in Fryer & Brown, 1986, where

$$\Delta x = [\ P_1\ (r^2 + 2x^2) + 2\ P_2\ xy\ ][\ 1 + P_3\ r^2 + \ldots] \quad (3)$$

$$\Delta y = [\ P_2\ (r^2 + 2y^2) + 2\ P_1\ xy\ ][\ 1 + P_3\ r^2 + \ldots] \quad (4)$$

where Δx and Δy are the decentering distortion values in the x and y coordinates respectively, and r is the radial distance. A conventional representation of decentering distortion is as a Profile function $P(r)$ where

$$P(r) = r^2\ (P_1^{\ 2} + P_2^{\ 2})^{1/2} \quad (5)$$

It is the profile function $P(r)$ which has been graphed in Figures 3 and 5 later in this paper. P_1 and P_2 may be easily determined from the plumbline method of lens calibration (Karara, 1989) or from a suitably rigorous bundle adjustment, as long as the correlation with offsets of the principal point have been duly acknowledged.

3.1.3 Offsets of the Principal Point: This characteristic of cameras is due to the imperfect alignment of the line of autocollimation to the centre of the image plane. The parameters representing this characteristic are conventionally referred to as x_p and y_p and as previously mentioned, are highly correlated to the decentering distortion parameters of P_1 and P_2. The values of x_p and y_p for each camera, as determined by the bundle adjustment, are shown in Table 4 in Section 5 of this paper.

3.1.4 Additional Parameters: The shear and tilt of sensor are represented by additional parameter terms from the following image coordinate correction equations (See Fraser, 1982).

$$\Delta x = \Delta x_1 + \Delta x_2 \quad (6)$$

$$\Delta y = \Delta y_1 + \Delta y_2 \quad (7)$$

where

$$\Delta x_1 = -x_p + (-\bar{x}/c)\,dc + K_1\,\bar{x}\,r^2 + K_2\,\bar{x}\,r^4 + K_3\,\bar{x}\,r^6 + P_1\,(3\,\bar{x}^2 + \bar{y}^2) + 2\,P_2\,\bar{x}\,\bar{y} \quad (8)$$

$$\Delta y_1 = -y_p + (-\bar{y}/c)\,dc + K_1\,\bar{y}\,r^2 + K_2\,\bar{y}\,r^4 + K_3\,\bar{y}\,r^6 + 2\,P_1\,\bar{x}\,\bar{y} + P_2\,(\bar{x}^2 + 3\,\bar{y}^2) \quad (9)$$

$$\Delta x_2 = a_1\,\bar{x}\,\bar{y} + a_2\,\bar{y}^2 + a_3\,\bar{x}^2\,\bar{y} + a_4\,\bar{x}\,\bar{y}^2 \quad (10)$$

$$\Delta y_2 = b_1\,\bar{x} + b_2\,\bar{y} + b_3\,\bar{x}\,\bar{y} + b_4\,\bar{x}^2 + b_5\,\bar{x}^2\,\bar{y} + b_6\,\bar{x}\,\bar{y}^2 \quad (11)$$

where c is the initial value for the focal length and dc is the required adjustment to that value and

$$\bar{x} = x - x_p \quad (12)$$

$$\bar{y} = y - y_p \quad (13)$$

The additional parameters determined in the bundle adjustment were a_1, b_1, b_2 and b_3.

3.2 Radiometric Corrections

The radiometric characteristics of digital cameras encompass aspects of the electronics and signal transmission involved in acquiring and converting the analog signal to the digital image. As these factors differ with the different type of camera, some characteristics are mainly found in analog video cameras with others mainly associated with digital still cameras.

Phase patterns (as described by Ge, 1993), line jitter and noise are radiometric characteristics associated with analog video cameras when used in conjunction with a frame grabber. These characteristics are all due to the signal transmission and sampling of the signal by the frame grabber when producing the digital image. The effects on the image can be reduced without requiring new or expensive equipment, by taking a series of images and averaging them (see Höflinger & Beyer, 1993). This approach was incorporated into the procedure as described in Section 4 of this paper.

Another consideration for analog video cameras is to ensure that they have been thoroughly warmed up before images are acquired (see Beyer, 1992). The time adopted for this procedure was 90 minutes.

Digital still cameras do not have the above problems, as the image is converted to digital format immediately within the camera. Image compression within digital still cameras allows the storage of a large number of images without the need to download them (up to 48 in the Apple QuickTake). Although this is a necessary and useful function, the compression techniques modify the image. The modifications are not noticeable to the human eye, but can affect the results from photogrammetric measurements. Digital still cameras usually provide the option of low resolution images (high compression) and high resolution images (low compression). All images taken for calibration purposes have been acquired as high resolution images.

4. PROCEDURE

The calibration procedure developed would best be described as a self-calibrating test range calibration, as opposed to laboratory or on-the-job calibration (as described by Osborn, 1994). A target plate was manufactured (see Figure 1), being very similar to target plates used recently in other calibration procedures (*for example:* Clarke *et al.*, 1995; van der Vlugt, 1995). However, instead of using relatively small targets (2mm dia) which would produce images of targets of 5-7 pixels diameter, the targets were larger (5mm dia) to produce images of up to 30 pixels diameter, depending on the object distance used (ranging from 0.8m to 1.5m). This approach follows that of Shortis *et al.*, (1995b), as it provides more reliable results for the centroiding of the targets.

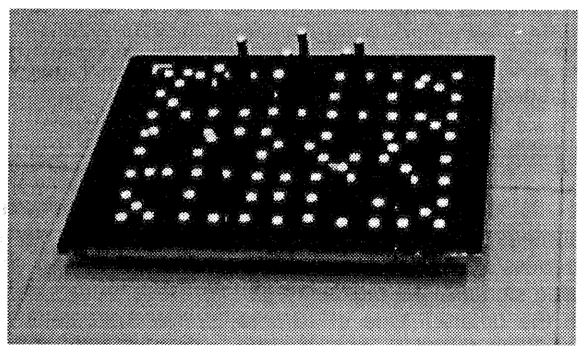

Figure 1. Target Plate.

The targets were punched from a sheet of retro-reflective material following research by Zumbrunn (1995), who showed that punching out the material was the preferred method of target manufacture. If a target is made by masking the retro-reflective material, the image of the target would be systematically shifted when viewed at a large angle (over 30°), thus making targets produced by that method unsuitable for this procedure.

The target plate was spray painted matt black to provide contrast to the retro-reflective targets. The effectiveness of this can be seen in Table 2 in Section 5 of this paper, which shows the background in the images (average minimum grey value) to be very low and the image of the targets (average maximum grey value) to be extremely high. The grey values (GV) can range from 0 to 255.

The target plate was coordinated using 1" theodolites to an accuracy determined to be 0.3mm. This was confirmed during the bundle adjustment and also by the photogrammetric tests of a fellow researcher (Mustaffar, 1995).

An extension to this target plate was constructed, to provide flexibility to accommodate the different focal lengths of the cameras. The original target plate as shown in Figure 1, fitted in the centre of the extension plate, which measured 700mm by 500mm. The calibration of the Philips cameras only required the original target plate to be imaged, whereas the Logitech Fotoman and the Apple QuickTake required the larger target plate to be used, due to their shorter focal lengths.

Images of the target plate were acquired using each of the four cameras to be calibrated. The images were acquired from nine different camera stations positioned around the target plate at 45° intervals and also from vertically above. The approach taken follows the self-calibration procedure described by Shortis *et al.*, (1995a).

For each of the two analog video cameras, the camera was set up on a tripod, warmed up for a sufficient period of time and then a set of ten images was taken at each of the nine camera stations. These images were averaged to provide a final set of images to be measured for use in the bundle adjustment. As a check, one set of the original images of the Right Philips was also measured to determine the effect of the averaging and is referred to in the results as Single Frame.

PC-based software programs were written to average the images, to make radiometric corrections to the images and to measure the image coordinates of the targets. A literature survey showed that there is usually no radiometric correction done to images after they have been acquired for errors such as pixels in the CCD array which show black when they should show white or the reverse.

As an adjunct to the calibration procedure, an investigation was carried out to determine whether corrections for such 'bad' pixels should be incorporated into the procedure. Such pixels could include isolated ones, blocks of pixels or the array as a whole not responding uniformly. This has been referred to as Non-Uniform Pixel Response by Beyer (1992). The result of the investigation is given in Section 5 of this paper.

A PC-based computer program (see Fryer, 1994 for a description) was used for the measurement of targets. The program was menu driven and displayed the digital image to be measured. To measure a target, the operator defined a rectangular area around the target, ensuring no other target encroached on that area. This area was processed to find the centroid of the target.

The centroiding involved accessing each grey value (GV) in the given window, finding the average GV and the maximum GV and establishing a threshold level. All pixels with a GV below the threshold level were ignored. The average threshold level for each target is shown for each camera in Table 2 in Section 5, along with the average number of pixels falling above the threshold level for each target.

Three different methods of weighting the pixels were used, being binary (BI), grey value (GV) and grey value squared (GV^2). The binary method applied a weight of one to each pixel, the grey value method weighted each pixel by its grey value and therefore, the brighter the grey value the more importance was put on the pixel. The grey value squared method used the square of the grey value at the weight to be applied, thus exaggerating the effect as described in the grey value method. Each method produced a separate set of observations and each was processed through the bundle adjustment. The results from each method have been tabulated in Section 5. However, only the binary results have been graphed in Figures 5, 6, 7 and 8 as the results from each method were very similar.

The program described above was customised to output files in the format compatible with the bundle adjustment being used. Three bundle adjustment programs were used initially for comparisons, with SPGA (Fraser, 1982) eventually being the sole bundle adjustment used as it was flexible, fast and efficient.

Prior to processing the observations in the bundle adjustment, the decentering distortion parameters P1 and P2 were determined using a plumbline lens calibration. These values were used as initial values in the bundle adjustment, to overcome the correlation problems with the offsets to the principal point, as previously mentioned.

5. RESULTS

The results from the calibration procedure have been tabulated and graphed in this section and include the calibration parameters for each camera, an analysis of the benefits of averaging images from video cameras, and an analysis of the benefits of radiometric corrections for 'bad' pixels and a comparison of the suitability of each camera for close-range photogrammetric measurement.

The calibration parameters for each camera are shown in Table 4. This table includes: the root mean square of the image coordinate errors in x and y; the focal length; the offsets to the principal point in x and y; lens distortion parameters K_1 , K_2 , P_1 and P_2 ; and the degrees of freedom from each bundle adjustment. From this table, it can be seen that the Single Frame of the Right Philips camera is only marginally worse in image coordinate RMS than the averaged binary, GV or GV squared, however, the averaging does improve the visual quality of the images, removing phase patterns and line jitter. The focal length was determined consistently for each camera. The Right Philips camera was shown to have a relatively large x component in the principal point offsets. The final values for P_1 as shown in Table 4 vary by only 5-10% from the initial values determined by the plumbline lens calibration.

The radiometric investigation, as described in Section 3.2, determined that there were no 'bad' pixels in these digital still cameras, and 'bad' pixels found in the analog video cameras were more due to sampling and signal transmission than problems in array. This was concluded after many images were acquired to find the 'bad' pixels in the video cameras, and the results were not consistent, but changed with each image.

The lens distortion parameters are graphed in Figures 5, 6, 7 and 8 in Section 5.3. The resultant values for the binary, grey value and grey value squared methods were all very similar, as can be seen in Table 4 and only the results of the binary method are graphed. The large radial distortion of the Apple Quicktake and the Logitech Fotoman should be noted. At a radial distance of 2mm, it is equivalent to a shift of 2 pixels, and at the edges of the array amounted to approximately 6 to 7 pixels. This would have to be considered when using the cameras for photogrammetric applications. Any targets or objects to be measured would best be situated close to the centre of the image to ensure the best results.

5.1 Statistical Results of Target Centroiding.

Camera	Average Maximum GV	Average Minimum GV	Average Threshold (0-255)	Pixels above Threshold
Left Philips	253.54	6.92	167.19	117.10
Right Philips	253.79	2.92	165.72	131.48
Apple Quicktake	254.55	1.18	159.76	24.19
Logitech Fotoman	255.00	12.76	170.98	29.38

Table 2. Statistical Results of Target Centroiding

As referred to in Section 4, Table 2 shows that the contrast between the targets (average maximum grey value) and the background (average minimum grey value) on the images was very high, which is beneficial for the centroiding of the targets.

5.2 Additional Parameters. See Section 3.1 for a mathematical description.

Camera	b_1	b_2	b_3	a_1
Left Philips				
Binary	0.246E-3	0.0298 **	0.452E-3	0.202E-2 *
GV	0.274E-3	0.0298 **	0.351E-3	0.221E-2 *
GV^2	0.259E-3	0.0298 **	0.427E-3	0.221E-2 *
Right Philips				
Binary	0.270E-3	0.0298 **	-0.302E-4	0.173E-2 *
GV	0.269E-3	0.0298 **	-0.859E-4	0.174E-2 *
GV^2	0.256E-3	0.0299 **	-0.721E-4	0.171E-2 *
Single Frame	0.112E-3	0.0298 **	0.137E-3	0.191E-2 *
Apple Quicktake				
Binary	0.273E-4	0.518E-4	-0.331E-4	-0.380E-4
GV	0.233E-4	0.448E-4	-0.210E-4	-0.484E-4
GV^2	0.267E-4	0.315E-4	0.249E-5	-0.418E-4
Logitech Fotoman				
Binary	0.698E-4	0.729E-4	-0.716E-4	-0.933E-4
GV	0.689E-4	0.752E-4	-0.815E-4	-0.894E-4
GV^2	0.716E-4	0.720E-4	-0.770E-4	-0.830E-4

* Significant ** Very Significant
(Significance determined by Fisher statistical analysis, see Fraser, 1982)
Table 3. Additional Parameters.

The most notable additional parameter in Table 3 is that of b_2 for the Philips cameras, showing that the actual size of the pixel in the y direction is 3% different from the initial value used.

5.3 Lens Distortions.

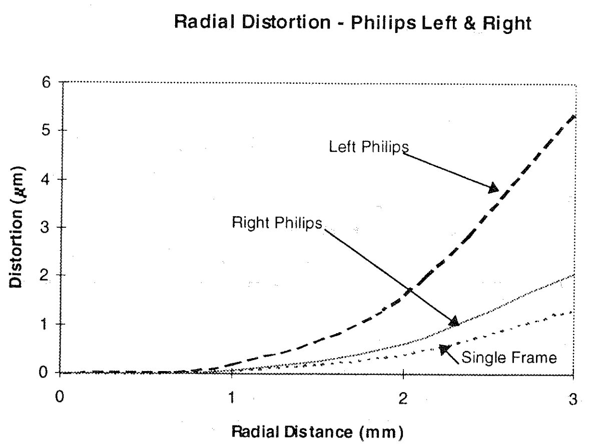

Figure 2. Radial Distortion - Philips Left, Right and Single Frame.

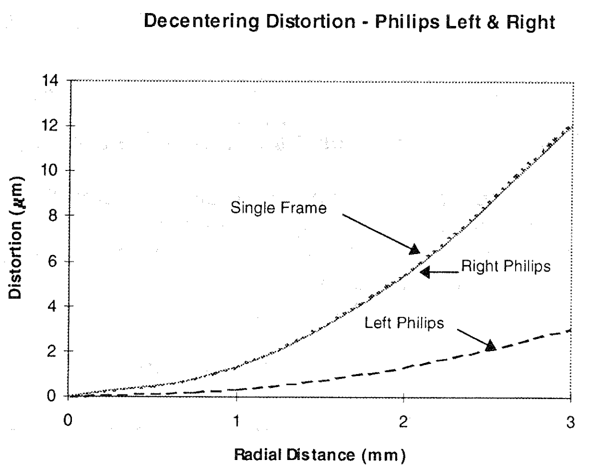

Figure 3. Decentering Distortion - Philips Left, Right and Single Frame.

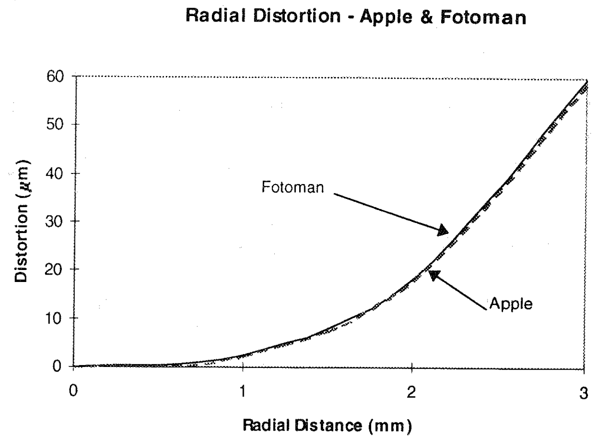

Figure 4. Radial Distortion - Apple and Fotoman.

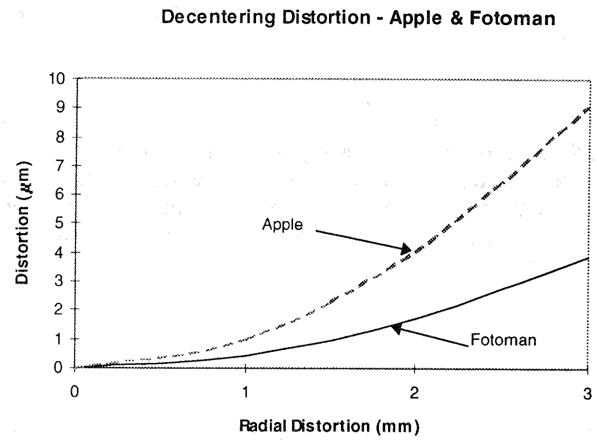

Figure 5. Decentering Distortion - Apple and Fotoman.

5.4 Camera Parameters.

Camera	Image RMS (x) (μm)	Image RMS (y) (μm)	Focal Length (mm)	x_p (mm)	y_p (mm)	K_1	K_2	P_1	P_2	Degrees of Freedom
Left Philips										
Binary	1.3	1.0	25.780	-0.006	0.062	0.201E-3	-0.132E-7	-0.108E-4	-0.336E-3	1300
GV	1.2	1.0	25.787	-0.009	0.061	0.216E-3	-0.420E-8	0.173E-4	-0.357E-3	1300
GV^2	1.2	0.9	25.785	-0.008	0.063	0.213E-3	0.136E-7	0.144E-4	-0.330E-3	1300
Right Philips										
Binary	1.2	0.9	25.718	-0.134	0.033	0.772E-4	-0.225E-7	0.132E-2	0.236E-3	1284
GV	1.2	0.8	25.709	-0.134	0.034	0.738E-4	-0.180E-7	0.133E-2	0.229E-3	1284
GV^2	1.2	0.8	25.713	-0.134	0.033	0.703E-4	-0.404E-8	0.133E-2	0.229E-3	1284
Single Frame	1.3	1.0	25.716	-0.126	0.042	0.498E-4	-0.235E-7	0.134E-2	0.224E-3	1284
Apple Quicktake										
Binary	1.0	0.9	8.327	0.061	0.002	0.223E-2	-0.724E-5	-0.963E-3	-0.291E-3	2398
GV	0.8	0.7	8.325	0.060	0.001	0.223E-2	-0.705E-5	-0.928E-3	-0.378E-3	2398
GV^2	0.7	0.6	8.323	0.060	0.000	0.222E-2	-0.668E-5	-0.904E-3	-0.456E-3	2398
Logitech Fotoman										
Binary	0.9	0.9	8.272	-0.079	0.010	0.234E-2	-0.141E-4	-0.375E-3	-0.214E-3	2452
GV	0.8	0.8	8.272	-0.079	0.010	0.234E-2	-0.123E-4	-0.378E-3	-0.201E-3	2452
GV^2	0.8	0.6	8.272	-0.081	0.010	0.233E-2	-0.116E-4	-0.374E-3	-0.183E-3	2452

Table 4. Camera Specifications

6. CONCLUSION

The aim of this research was to develop and apply a flexible camera calibration procedure which could easily accommodate different types of cameras. This was successfully achieved and the procedure was applied to four different cameras. Two analog video cameras were tested with a frame grabber. The radiometric difficulties associated with the camera/frame grabber combination were overcome, to a large extent, by averaging the images. In the case of the digital still cameras, the advantages of not having the radiometric problems are offset by the use of obviously cheaper lenses which have large radial distortions. This should be a consideration when using this type of camera for photogrammetric applications.

7. ACKNOWLEDGEMENTS

I would like to thank Professor John Fryer for his advice on camera calibration. The program for the measurement of the coordinates was written by Dr Eric Kniest, University of Newcastle, Australia.

8. REFERENCES

Beyer, H.A., 1992. Geometric and Radiometric Analysis of a CCD Camera based on a Photogrammetric Close-Range System. Thesis, Institute for Geodesy and Photogrammetry, Zurich, 186 pages.

Burner, A.W., Snow, W., Shortis, M., & Goad, W., 1990. Laboratory Calibration & Characterisation of Video Cameras. 'Close Range Photogrammetry Meets Machine Vision', SPIE, Vol 1395, pp 664-671.

Clarke, T., Cooper, M., Chen, J. & Robson, S., 1995. Automated Three Dimensional Measurement using Multiple CCD Camera Views. Photogrammetric Record, 15(85), pp 27-42.

Curry, S., Baumrind, S., & Anderson, J., 1986. Calibration of an Array Camera. Photogrammetric Engineering & Remote Sensing, 52(5), pp 627-636.

Fraser, C., 1982. On the Use of Nonmetric Cameras in Analytical Close-Range Photogrammetry. The Canadian Surveyor, 36(3), pp 259-279.

Fryer, J., 1994. Teaching Photogrammetry with a Simple Digital Camera. International Archives of Photogrammetry & Remote Sensing, 30(6), Commission VI, Beijing, 5 pages.

Fryer, J. & Brown, D., 1986. Lens Distortion for Close-Range Photogrammetry. Photogrammetric Engineering and Remote Sensing, 52(1), pp 51-58.

Fryer, J. & Fraser, C., 1986. On the Calibration of Underwater Cameras. Photogrammetric Record, 12(67), pp 73-85.

Ge, R., 1993. Line Jitter Detection of CCD Cameras. Optical 3D Measurement Techniques II, Zurich, Gruen & Kahmen (editors), Wichmann, Karlsruhe, pp 239-246.

Höflinger, W., & Beyer, H., 1993. Characterisation & Calibration of a S-VHS Camcorder for Digital Photogrammetry. Optical 3D Measurement Techniques II, Zurich, Gruen & Kahmen (editors), Wichmann, Karlsruhe, pp 133-140.

Karara, H. (editor), 1989. Handbook of Non-Topographic Photogrammetry. Second Edition. ASPRS, Virginia, pp 59-69.

Lenz, R., 1987. Lens Distortion Corrected CCD Camera Calibration with Co-planar Calibration Points for Real-Time 3D Measurements. Proceedings of ISPRS Intercommission Conference on Fast Processing of Photogrammetric Data, Interlaken, Switzerland, pp 60-67.

Michael, D., 1992. Camera Calibration Using Postscript Interference Patterns. Videometrics, SPIE, Vol 1820, pp 9-15.

Mustaffar, M., 1995. Personal communication.

Osborn, J., 1994. Design and Calibration of Close-Range Stereophotogrammetric Systems in Biology and Biomedicine. Ph.D. Thesis, Department of Surveying and Spatial Information Science, University of Tasmania, Australia, 365 pages.

Shortis, M., & Snow, W., 1995a. Calibration of CCD Cameras for Field and Frame Capture Modes. Conference on Digital Photogrammetry and Remote Sensing, St Petersburg-Great Lakes, Russia, 11 pages.

Shortis, M., Snow, W. & Goad, W., 1995b. Comparative Geometric Tests of Industrial & Scientific CCD Cameras using Plumb Line and Test Range Calibrations. International Archives of Photogrammetry & Remote Sensing, 30(5W1), 'From Pixels to Sequences', Zurich, Switzerland, pp 53-59.

van der Vlugt, G., 1995. Algorithms and Design Aspects of an Automated Vision Based 3-D Surface Measurement System. Ph.D. Thesis, University of CapeTown, South Africa, 132 pages.

Wong, Kam & Obaidat, M., 1994. CCD Camera Calibration using Planar Constraint. International Archives of Photogrammetry & Remote Sensing, 30(5), Proceedings of Commission V, Australia, pp 447-451.

Zumbrunn, R., 1995. Systematic Pointing Errors with Retro-Reflective Targets. International Archives of Photogrammetry & Remote Sensing, 30(5W1), 'From Pixels to Sequences', Zurich, Switzerland, pp 60-65.